JOURNAL OF AGRICULTURAL AND FOOD CHEMISTRY

ARTICLE

pubs.acs.org/JAFC

Food Volatile Compounds Facilitating H_{II} Mesophase Formation: Solubilization and Stability

Natali Amar-Zrihen, Abraham Aserin, and Nissim Garti*

The Ratner Chair of Chemistry, Casali Institute of Applied Chemistry, The Institute of Chemistry, The Hebrew University of Jerusalem, Edmond J. Safra Campus, Givat Ram, Jerusalem 91904, Israel

ABSTRACT: Four lipophilic food volatile molecules of different chemical characteristics, phenylacetaldehyde, 2,6-dimethyl-5-heptenal, linalool, and *trans*-4-decenal, were solubilized into binary mixtures of monoolein/water, facilitating the formation of reverse hexagonal (H_{II}) mesophases at room temperature without the need of solvents or triglycerides. Some of the flavor compounds are important building blocks of the hexagonal mesostructure, preventing phase transition with aging. The solubilization loads were relatively high: 12.6, 10.0, 12.6, and 10.0 wt % for phenylacetaldehyde, 2,6-dimethyl-5-heptenal, linalool, and *trans*-4-decenal, respectively. Phenylacetaldehyde formed mixtures of lamellar and cubic phases. Linalool, 2,6-dimethyl-5-heptenal, and *trans*-4-decenal induced structural shift from lamellar directly to H_{II} mesophase, remaining stable at room temperature. Lattice parameters were found to increase with water content and to decrease with temperature and/or food volatile content. *trans*-4-Decenal produces more stable H_{II} mesophase compared to linalool-loaded mesophase. At 40−60 °C, depending on the chemical structure and on the solubilization location of the food volatile compounds, the H_{II} mesophase transforms to isotropic micellar phase, facilitating the release of the food volatile compounds. Molecular interactions suggest the existence of two consecutive stages in the solubilization process.

KEYWORDS: monoolein, linalool, melonal, decenal, phenylacetaldehyde, lyotropic liquid crystals

INTRODUCTION

Monoglycerides of fatty acids in aqueous systems spontaneously self-assemble into various lyotropic liquid crystalline (LLC) structures. These mesophases are characterized by high symmetry, large interfacial area, and both hydrophilic and lipophilic domains.[1−4] Three well-established classes of LLC phases, lamellar (L_α), hexagonal [normal (H_I) or inverted (H_{II})], and normal or inverted cubic [bicontinuous (V_I, V_{II}) or micellar (I_I, I_{II})][5−7] are well characterized. Some of the most established disordered structures are of discontinuous cubic micellar (I) and sponge phases (L_3 and L_4).[6,7] Recently, we prepared a discontinuous cubic micellar reverse mesophase (Q_L) with unique fluid characteristics.[8] The level of order of each mesophase depends on the content of the lipophilic "oil phase" and on other external physical parameters such as pH, temperature, and pressure.[9−13] Other factors affecting the mesophase structure are the molecular shape of the surfactant, packing parameter, and interfacial curvature energy.[14−19]

The physical properties of reverse hexagonal liquid crystals (H_{II}) are less studied compared with those of cubic and lamellar phases.[20−22] The reverse hexagonal mesophase is characterized by dense packing of infinitely long rods and exhibits 2D ordering. The hexagonal unit cell is of a primitive (*P6mm*) type, which symbolizes one long rod per unit cell corner (Figure 1). The H_{II} phase of monoolein/water exists only at elevated temperatures (85 °C). Triacylglycerols (triglycerides, TAG), mainly tricaprylin, were added to the binary mixture of monoolein/water to promote the formation of H_{II} phases at room temperature.[23−27]

The morphology of the LLC that is formed upon addition of triglycerides is affected by the guest molecule geometry. This geometrical effect can be envisaged through the critical packing parameter, CPP = $V_S/a_0\,l$, where V_S is the hydrophobic chain volume, a_0 is the cross polar headgroup area, and l is the chain length of the molecule in its molten state.[14] It is known that reversed-type mesophases are formed from amphiphiles with CPP > 1. For the GMO/water system, the packing parameters of L_α, Q_L and H_{II} mesophases are 1.0, 1.3, and 1.7, respectively.[24,25] The TAG molecules spaced the tails of the GMO, and an effective CPP of *ca.* 1.7 was probably obtained.[14,24,25] These room temperature stable mesophases were considered as potential drug delivery vehicles.[28−38]

In recent years, self-assembled mesophases into which various bioactive compounds were solubilized provide significant functionality and health benefits in food systems.[39−41] Lyotropic mesophases are considered to be delivery and controlled release vehicles for many possible active ingredients.[15,42−45] Vauthey et al. used LLC as microreactors for the synthesis of flavor compounds,[46] to release some of them from cubic and micellar mesophase, and to demonstrate the advantages of these mesophases over emulsions and microemulsions.[47]

Phenylacetaldehyde, 2,6-dimethyl-5-heptenal, linalool, and *trans*-4-decenal are four hydrophobic food volatile molecules with major oxidation and degradation sensitivity once exposed to air (Figure 2). The studied molecules belong to the ***nature-identical*** class, which are produced synthetically but are chemically identical to their natural counterparts and serve as fragrance and flavor additives.[48] They are usually stored at low temperatures, in the

Received: February 3, 2011
Revised: April 12, 2011
Accepted: April 16, 2011
Published: April 16, 2011

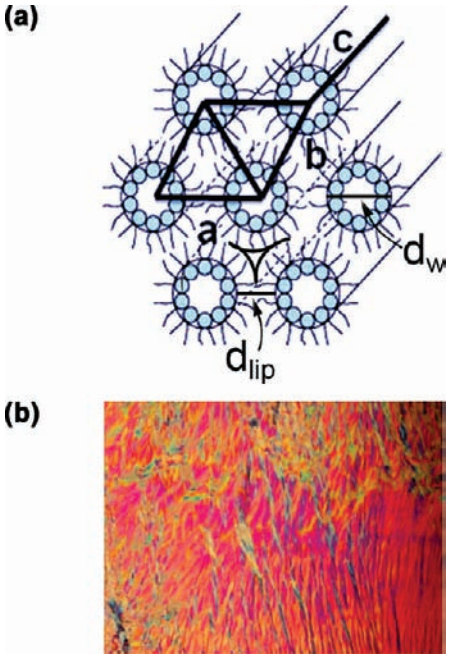

Figure 1. (a) Schematic illustration of the geometry of the reverse hexagonal mesophase packing of inverted cylinders. The unit cell can be visualized in terms of three sides of the cell: *a*, *b*, and *c*, where $a = b$ is the space between each corner of the cylindrical micelles (termed the lattice parameter *a*), and *c* is the infinite length of each rod; d_{lip} is the distance of the lipid layer between two adjacent rods, and d_w is the diameter of the water channel of the rods. (b) Typical polarizing microscopy image of the hexagonal mesophase at 25 °C.

dark, and under nitrogen. These four molecules have moderate volatility, are soluble in vegetable oils, and belong to the flowery-fruity aroma group.

The main goal of this study is to demonstrate that these food volatile molecules can be solubilized at the lipid or interfacial layer of the mesophase and be protected and released at will. In this study we scrutinized their solubilization capacities as well as their structural capabilities to stabilize formation of reversed hexagonal mesophase at room temperature without the need for TAG compounds, which are not required for the current application.

The effect of temperature on the lattice parameter as an indication of the location of the food volatile molecules within the interface, and on the transformation of hexagonal to micellar mesophase as an indication of the release properties of these compounds, was determined.

MATERIALS AND METHODS

Chemicals. Distilled monoolein (distilled glycerol monooleate, GMO) consisting of 97.1 wt % monoglycerides, 2.5 wt % diglycerides, and 0.4 wt % free glycerol (acid value, 1.2; iodine value, 68.0; melting point, 37.5 °C) was obtained from Riken Vitamin Co. Ltd., Tokyo, Japan; linalool, *trans*-4-decenal, 2,6-dimethyl-5-heptenal (melonal), and phenylacetaldehyde were obtained from Frutarom Ltd., Haifa, Israel (minimum 95% purity). Tricaprylin (triacylglycerols, TAG; assay, 97−98%) was obtained from Sigma Chemical Co. (St. Louis, MO). The water was double distilled. D_2O (D, 99.9%) was purchased from Cambridge Isotope Laboratories Inc., Andover, MA. All ingredients were used without further purification.

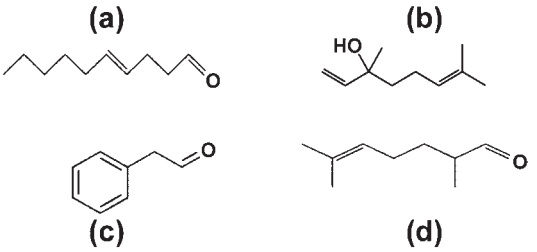

Figure 2. Chemical structures of (a) *trans*-4-decenal, (b) linalool, (c) phenylacetaldehyde, and (d) 2,6-dimethyl-5-heptenal (melonal).

Preparation of H_{II} Mesophases. To determine the solubilization behavior and solubilization efficacy of these food volatile molecules, a ternary phase diagram (GMO/water/food volatile compound) was prepared. The phase diagram was built up in the following way: mixtures of the three components were prepared at different weight ratios of food volatile molecules to GMO to water. Each phase diagram can be divided into dilution lines, where each dilution line represents a constant ratio between food volatile compound and GMO and a variable water concentration (0−30 wt%). All samples were kept in culture tubes sealed (under nitrogen atmosphere to avoid oxidation) with Viton-lined screw caps, heated to a maximum of 70 °C for a duration of 10 min, slightly vortexed for no more than 1 min, and kept in a 25 ± 0.5 °C water bath. The samples were allowed to equilibrate for 48 h before they were examined. The different mesophases were determined using an optical cross-polarized microscope and SAXS methods.

Optical Microscope. Preliminary structure examination through a cross-polarized light microscope was implemented to distinguish between typical mesophases according to their characteristic textures.[25] Microscopic observations were performed using two different light microscopes: (1) A Nikon model Eclipse 80i microscope was equipped with Nikon Digital Imaging Head with Fluorescence and Imaging Capabilities, Nikon Digital Camera model DXM 1200C, and Nikon X-cite Series120 Illuminator (Tokyo, Japan). The samples were analyzed at room temperature. (2) Mesophase transitions as a function of the temperature were viewed through a Nikon optical microscope (Nikon AFX-IIA, Tokyo, Japan) equipped with cross-polarizers, a Nikon FX 35 WA camera, and with a Mettler FP82 hot stage (Greifensee, Switzerland) and then heated and/or cooled at a rate of 5 °C/min.

Small-Angle X-ray Scattering (SAXS). Further structure clarification was conducted by SAXS measurements to distinguish between the different mesophases by their Bragg peak *d*-spacing ratio. Scattering experiments were performed using Ni-filtered Cu K_α radiation (0.154) from a Philips sealed tube X-ray generator that operated at a power rating up to 1.36 kW. X-radiation was further monochromated and collimated by a single Franks mirror and a series of slits and height limiters and measured by a linear position-sensitive detector. The samples were inserted into 1.5 mm quartz capillaries. The temperatures were maintained at $T \pm 0.5$ °C. The sample to detector distance was 0.46 m, and the scattering patterns were smeared using the Lake procedure implemented in home-written software.[49]

Differential Scanning Calorimetry (DSC). A Mettler Toledo DSC822 (Greifensee, Switzerland) calorimeter was used. The DSC measurements were carried out as follows: 5−15 mg LLC samples were weighed, using a Mettler M3 microbalance, in standard 40 μL aluminum pans and immediately sealed by a press. The samples were rapidly cooled in liquid nitrogen from 25 to −40 °C, at a rate of 10 °C min^{-1}. The samples remained at this temperature for 30 min and then were heated at 1 °C min^{-1} to 40 °C. An empty pan was used as reference. The instrument determined the fusion temperatures of the solid components and the total heat transferred in any of the observed thermal processes. The enthalpy change associated with each thermal transition was obtained by

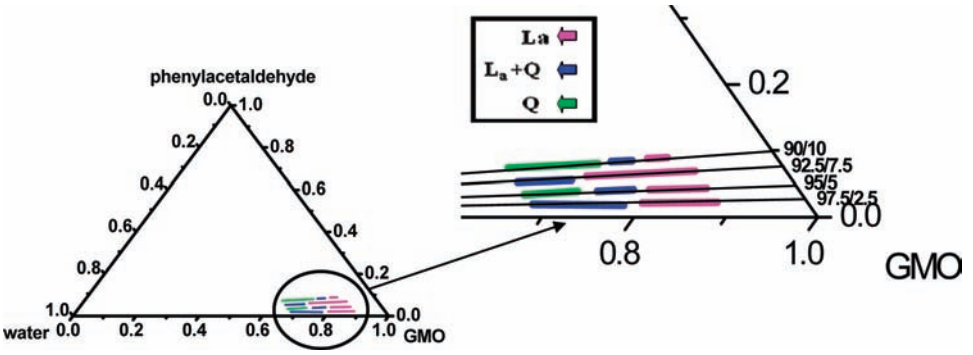

Figure 3. Ternary phase diagram of GMO/phenylacetaldehyde/water at 25 °C. The dilution lines represent the surfactant/phenylacetaldehyde weight ratio.

integrating the area of the relevant DSC peak. DSC temperatures and enthalpy results reported here were reproducible to ±0.2 °C and ±2%, respectively.

Attenuated Total Reflectance-Fourier Transform Infrared (ATR-FTIR) Measurements. An Alpha P model spectrometer, equipped with a single-reflection diamond ATR sampling module, manufactured by Bruker Optik GmbH (Ettlingen, Germany), was used to record the FTIR spectra. The spectra were recorded with 50 scans, at 25 °C; a spectral resolution of 2 cm^{-1} was obtained.

ATR-FTIR Data Analysis. Multi-Gaussian fitting has been utilized to resolve individual bands in the spectra. The peaks were analyzed in terms of peak wavenumbers, width at half-height, and area. The ATR-FTIR measurements were conducted with D_2O replacing the water to avoid a hydroxyl stretching band overlapping with the GMO hydroxyl bands.

Gas Chromatography. The food volatile molecules loaded into the H_{II} mesophase were analyzed using a gas chromatograph with standard solutions of each volatile compound diluted with hexane. Chromatographic measurements were performed with the GC-MS system on a 5890 gas chromatograph (Hewlett-Packard, USA), fitted with a splitless injector intended for use with capillary columns and a mass spectrometer. The ionization source was of an electron impact (EI) mode. The GC-MS was operated using helium as the carrier gas with a flow rate of 1 mL min^{-1}. Two microliters of the analyzed solution was injected into a DB-5MS capillary fused silica column (0.25 mm diameter, 30 m length, 0.25 μm film thickness), and the injector temperature was set to 290 °C. The column temperature was programmed after 2 min to increase from 60 to 170 °C at 2 °C min^{-1} and further increased to 300 °C at 15 °C min^{-1}. Recording of the EI mass spectra was conducted with a scan range of 50−500 amu. The obtained data were processed using the GC-MS ChemStation software package.

RESULTS AND DISCUSSION

Transitions to H_{II} Mesophases Induced by Solubilized Food Volatile Compounds. As a first goal in this work we explored the possibility of using the food volatile compounds as substitutes for the TAG molecules in an attempt to form the hexagonal mesophase at room temperature. It was assumed that these molecules, being mostly lipophilic and consisting of a medium chain length lipophilic moiety, will space the tails of the monoolein molecules and will influence the CPP of the GMO.

At first we scrutinized the incorporation and solubilization capacities of the food volatile compounds in the GMO/water system. It was assumed that the H_{II} mesophase will be stabilized at room temperature. $L_\alpha \rightarrow H_{II}$ and $Q \rightarrow H_{II}$ transitions were expected to occur in the presence of the food volatile molecules. Ternary phase diagrams in a similar compositional range (rich in monoolein) were constructed in which the TAG was totally replaced.

GMO/Water/Phenylacetaldehyde Ternary Mixtures. At 90/10 GMO/water weight ratio (90 wt % GMO and 10 wt % water) up to 10 wt % of phenylacetaldehyde was solubilized. This means a molar ratio of GMO/phenylacetaldehyde of 3/1. Only lamellar and cubic structures were formed (Figure 3), similar to what was obtained in the binary mixture of GMO/water without phenylacetaldehyde.[25] The parameters to differentiate each mesophase were described in detail in the literature[1,2] and in our previous works.[8,25−29,39] As the phenylacetaldehyde part of the molecules was too short, it did not induce transition to hexagonal mesophase. Close examination of the effect of the phenylacetaldehyde content on the mesophase reveals there are at least three different structures that can be formed depending on the water content and the GMO/water ratio. The dominant structure is the lamellar, next (with more water added) is a mixture of lamellar and cubic mesophases, and in the presence of additional quantities of water a third region of cubic mesophase was formed.

In the monoolein-rich, and in relatively water-poor, regions (0−30 wt %), a well-defined pure lamellar structure was formed within all four water dilution lines (confirmed by SAXS and microscope), but once more water was added, mixtures of cubic and lamellar mesophases were detected. Yet, eventually (above 24 wt % water), once the concentration of the monoolein was reduced (water dilution line 90/10, Figure 3) cubic mesophase was formed (SAXS). This indicates that the effective CPP in the presence of water excess (less monoolein) and phenylacetaldehyde increases slightly only to *ca.* 1.3. The phenylacetaldehyde does not space the tails sufficiently to achieve an effective CPP of *ca.* 1.7, which is needed to form reverse hexagonal mesophase.

GMO/Water/Food Volatile Compound Ternary Mixtures. The other three food volatile compounds are easily incorporated into the binary mixture with maximum solubilization capacities of 12.6, 10.0, and 12.6 wt % for 2,6-dimethyl-5-heptenal, linalool, and *trans*-4-decenal, respectively (molar ratios of GMO to each of the food volatiles are 2.65, 3.68, and 3.0, respectively, for the corresponding GMO/water dilution lines of 85/15, 85/15, and 87.5/12.5).

Solubilization of 2,6-dimethyl-5-heptenal, linalool, and *trans*-4-decenal into the binary mixture facilitated the formation of H_{II} mesophase. The food volatile compounds transformed the lamellar, or the cubic, mesophases directly to reverse hexagonal mesostructure at room temperature. The food volatile molecules modified the CPP of the monoolein to *ca.* 1.7 and allowed structuring of

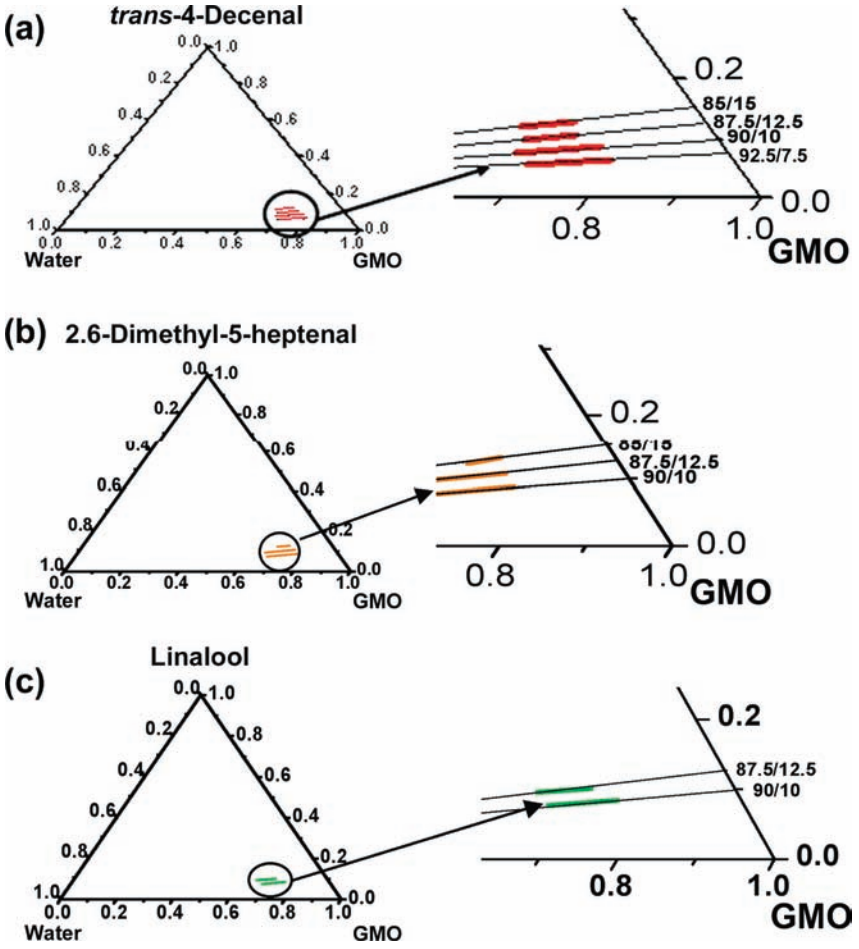

Figure 4. Partial ternary phase diagrams of GMO/water and (a) *trans*-4-decenal, (b) 2,6-dimethyl-5-heptenal (melonal), and (c) linalool at 25 °C. The dilution lines represent the surfactant/food volatile compound weight ratio.

the H_{II} at room temperature even in high or low water and high or low GMO contents.

The H_{II} mesostructure was identified using two classical techniques, cross-polarized optical microscope ("fan" type texture) and SAXS diffractions (three Bragg peaks with the ratio $1:\sqrt{3}:\sqrt{4}$, corresponding to the reflections from the dense packing of cylindrical micelles arranged on a 2D-hexagonal symmetry).[1,2]

Transition to H_{II} mesophases by *trans*-4-decenal, 2,6-dimethyl-5-heptenal, and linalool occurred at 5.5−12.6, 7.5−12.6, and 7−10 wt %, respectively (Figure 4). The three food volatile molecules are efficiently incorporated between the monoolein hydrophobic chains and facilitate the formation of reverse hexagonal mesophase, without the need for excess water or triglycerides.

The effect of *trans*-4-decenal is demonstrated in two water contents (Figure 4a). In the binary system, at 15 wt % water, lamellar liquid crystals are usually formed. However, at equal water content, in the presence of 5.5−12.6 wt % *trans*-4-decenal (up to GMO/*trans*-4-decenal ratio of 85/15) a reversed hexagonal mesostructure was detected. At 20 wt % water in binary systems usually a mixture of lamellar and cubic phases is formed; however, in the presence of 6−11.5 wt % *trans*-4-decenal, a reversed hexagonal mesophase is observed.

Although the smallest range of hexagonal mesostructure was observed by the solubilization of linalool (Figure 4c), this compound was the only one that already at 16 wt % water caused phase transition to H_{II} ($L_\alpha \rightarrow H_{II}$), compared to the binary system in which only lamellar phase was formed.

trans-4-Decenal was found to be the most effective (with more compositional options) in altering the CPP value of the monoolein and inducing the formation of reverse hexagonal liquid crystals. Figure 4a shows the ternary phase diagram of GMO, *trans*-4-decenal, and water with the largest area of reversed hexagonal phase. This large region of reverse hexagonal mesophase was detected even with as low as 5.5 wt % *trans*-4-decenal in water dilution line 92.5/7.5 (in the presence of 14−25 wt % water) and up to a maximum concentration of 12.6 wt % *trans*-4-decenal in water dilution line 85/15 (in the presence of 16−23 wt % water).

This behavior is very relevant in the design of food products because it allows the formulator to use, at will, systems rich or poor in water with low and high loads of food volatile compounds.

Sjölund et al. examined the effect of *n*-alkanes on a phosphatidylcholine−water system and found that the alkanes are able to induce phase transitions.[50] One assumes that specific phase formation is associated with an optimum chain length and that deviation from this length costs the free energy of stretching or compressing the chains. In the L_α mesophase, the chains are all of the same average length, and this contribution is small. However, in the H_{II} mesophase, there is a systematic variation in chain length around the H_{II} tube (Figure 1a) that raises the free energy

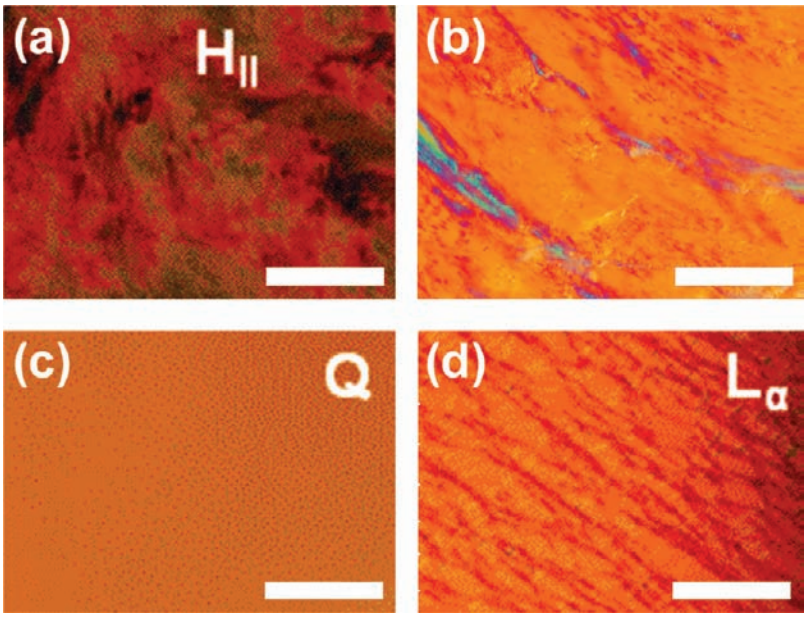

Figure 5. LLC polarizing microscopy images containing 8.6 wt % 2,6-dimethyl-5-heptenal (melonal) in 90/10 water dilution line (GMO/2,6-dimethyl-5-heptenal ratio) after (a) 1 day (hexagonal phase), (b) 3 days (transition state), (c) 1 week (cubic phase), and (d) 2 weeks (lamellar phase). The scale bar is 150 μm.

of this geometry.[51] Furthermore, the water cylinder of the H_{II} mesophase is large and increases with water content; the bending of the lipid monolayer will create void volumes in the hydrophobic regions. Thus, lipid packing constraints and low water content in the system will prevent the formation of lipid aggregates with large radii of curvature. However, by the theory of Gruner et al., hydrophobic guest molecules (such as alkanes) can remove these constraints by allowing the formation of large water cylinders and filling the void volumes between the cylinders in the H_{II} mesophase.[52,53] These two explanations might apply to our case because the bending of the interfacial layer is essential to obtain the required CPP of the hexagonal mesophase and the low water content prevents aggregation of large aggregates with larger radii. The hexagonal mesophase is formed in the presence of the proper structure of the food volatile compounds that comply with these requirements and brings the CPP to its required value.

From these two theories we can conclude that phenylacetaldehyde probably could only partially fill the void volumes or hydrate the monoolein headgroup; hence, it only slightly increases the CPP and induces $L_\alpha \rightarrow Q$ transformation. However, it cannot form hexagonal structures, even at high concentrations. Linalool and *trans*-4-decenal molecules are sufficiently incorporated between the GMO hydrophobic chains and fill the void volumes; therefore, they were able to dramatically affect the CPP and R_0 values without any dependence on temperature (as in the binary diagram). As a result of their effective incorporation, they transform the lamellar mesophase directly to hexagonal mesophase, and not *via* cubic mesophase.

Solubilization of 7.5 wt % 2,6-dimethyl-5-heptenal into the binary system induces phase transition from lamellar to hexagonal liquid crystal (Figure 4b). However, these liquid crystals were found to be nonthermodynamically stable, and after 2 weeks a back transition from hexagonal to lamellar *via* cubic mesophase was observed (Figure 5).

Considering the fact that 2,6-dimethyl-5-heptenal and *trans*-4-decenal molecules are structurally similar, we would expect the same behavior. The reason for obtaining these differences in their behavior might be derived from steric hindrance of the 2,6-dimethyl-5-heptenal methyl group positioned alpha to the carbonyl, which disturbs the entrapment of the molecule into the interface. These molecules, although they have enlarged monoolein tail volumes and as a result also effective CPP (ECPP),[25,54] are supersaturated at the interface and have a tendency with time (2 weeks) to migrate out of the interface, causing a reverse transition to its original preferred organization. ECPP is the sum of the volumes of all the surfactants, cosurfactants, and other molecules participating at the interface divided by the product of the sum of the areas of the headgroups with the sum of the lengths of the tails.[54]

It was demonstrated that all examined guest molecules except phenylacetaldehyde cause a transformation from lamellar (or cubic) to H_{II}. The tendency of the different food volatile compounds to induce phase transition can be explained thermodynamically and in terms of the geometry effect (ECPP) of the guest molecules that are derived from their interactions around the headgroups of the monoolein (phenylacetaldehyde) or on its tails (*trans*-4-decenal and linalool).

We selected the two best transition-inducing food volatile molecules for studying the molecular and structural characteristics of the mesophases (*trans*-4-decenal and linalool).

Structural Properties. The lattice parameter dependence on composition of the mesophase along dilution lines of two of the food volatile molecules was examined by SAXS.

Generally, the guest molecules can interfere with the structure and the effective packing parameter within three regions of the GMO molecular structure: next to the headgroup (hydroxyl groups), close to interface (its carboxyl group), and within the tails (fatty acid chains). The solubilized molecules that are located close to the headgroups compete for water hydration, dehydrate the hydroxyl groups, and pack them more closely together (reducing the headgroup cross-section area), increasing the CPP. In addition, the effect of the food volatile tails is also

Table 1. Effect of Food Volatile Guest Molecules on the Lattice Parameter (α) in GMO/Linalool/Water and GMO/*trans*-4-Decenal/Water Systems at Dilution Line 90/10

	lattice parameter α[a] (Å)	
water content (wt %)	GMO/linalool/water	GMO/*trans*-4-decenal/water
18	52.7	53.3
20	53.3	54.4
22	54.4	54.9
24	56.2	60.9

[a] α ± 0.5 Å.

significant, increasing the volume GMO of the tails (larger V_S in the CPP equation). These effects cause mesophases to transform to hexagonal mesophases and to increase the ECPP. This causes a larger lipid layer, d_{lipid} (Figure 1a), and hence increases the lattice parameter (more space between the tails). Once the hexagonal phase is formed, the food volatile compounds enlarge the lattice because they facilitate entrapment of more water with larger channels, d_w.

These effects are expected from food volatile compounds that consist of functional carbonyl groups and lipophilic tails. The end result is an enlargement of the lattice parameter with increasing water content (Table 1). It is expected that the swelling effect is more dominant than the dehydration or volume effects.

Comparing the systems based on *trans*-4-decenal to those of linalool shows that the first has a stronger enlarging lattice parameter effect than the second. We can assume that the difference is attributed to the different location of the food volatile compounds within the *trans*-4-decenal molecule, which has a stronger tail spacing effect than the linalool, and the combined lipophilic layer effect with the welling effect leads to a stronger lattice parameter increase.

In addition, at 18 wt % water (dilution line 90/10), the lattice parameter is ∼53 Å in the presence of either *trans*-4-decenal or linalool. However, with greater water content (24 wt %), when there is sufficient water to hydrate the monoolein polar headgroups to form highly ordered structures, the effect of the food volatile guest molecule on the lattice parameter is more pronounced. As shown in Figure 1a, the shaded area (triangle) represents an interstice (void) whose volume must be filled with the GMO hydrophobic chains and/or lipophilic guest molecules (food volatile molecule). This volume is determined to be 0.0931 of the unit-cell volume after subtraction of the volume occupied by the maximum-sized circular cylinders of α/2 from the unit-cell volume.[55] High water content will not influence the miscibility of the guest molecule into the lipid but will increase the lipid−water cylinder radius (Table 1) and, therefore, also the volumes between the cylinders. When the water content is augmented, looser structures are formed; therefore, the lattice parameter is more sensitive to modifications in the system such as addition of a third component that fills the void.

Effect of Food Volatile Molecule Concentration on Lattice Parameter. The concentration effect of the solubilized food volatile molecule on the lattice parameter was examined by focusing on the GMO/*trans*-4-decenal/water system, because it has the largest hexagonal region. Table 2 shows lattice parameter values of the hexagonal mesophase containing *trans*-4-decenal in several water dilution lines at 14−24 wt % water.

Table 2. Effect of *trans*-4-Decenal and GMO Contents on the Lattice Parameter (α) in Ternary Mixtures of GMO/*trans*-4-Decenal/Water (at Different Water Dilution Lines)

water dilution line	water (wt %)	GMO (wt %)	*trans*-4-decenal (wt %)	α[a] (Å)
92.5/7.5	14	79.6	6.5	50.3
90/10	14	77.4	8.6	51.6
92.5/7.5	16	77.7	6.3	50.5
90/10	16	75.6	8.4	52.2
87.5/12.5	16	73.5	10.5	49.6
85/15	16	71.4	12.6	49.4
92.5/7.5	18	75.9	6.2	55.1
90/10	18	73.8	8.2	53.3
87.5/12.5	18	71.8	10.3	53.7
85/15	18	69.7	12.3	52.7
92.5/7.5	20	74.0	6.0	55.4
90/10	20	72.0	8.0	56.7
87.5/12.5	20	70.0	10.0	54.4
85/15	20	68.0	12.0	52.4
92.5/7.5	22	72.2	5.8	60.6
90/10	22	70.2	7.8	55.0
87.5/12.5	22	68.3	9.8	56.8
85/15	22	66.3	11.7	53.0
92.5/7.5	24	70.3	5.7	61.0
90/10	24	68.4	7.6	60.9

[a] α ± 0.5 Å.

At low water content and high monoolein content the increase in *trans*-4-decenal solubilization content (6.5−8.6 wt % *trans*-4-decenal) in water at dilution lines 92.5/7.5 and 90/10 did not significantly change the lattice parameter (from 50.3 to 51.6 ± 0.5 Å, respectively). At 16, 18, and 20 wt % water, the GMO content decreased slightly, and the lattice parameter also decreased slightly (from 50.5, 55.1, and 55.4 ± 0.5 Å to 49.4, 52.7, and 52.4 ± 0.5 Å, respectively. All reductions in the lattice are relatively small but consistently more significant as the water content increases.

The effect of food volatile molecule concentration is the most pronounced at high water concentrations. At 22 wt % water well-defined packing of the micelles is expected; an increase in the *trans*-4-decenal concentration (and decrease in GMO content) yielded more disordered structures with smaller aggregation numbers (number of molecules at the interface) and thus the lattice parameter shrunk from 60.6 to 53.0 ± 0.5 Å. At 24 wt % water the system is oversaturated; thus, no significant decrease in the lattice parameter was observed by increasing the concentration of the food volatile molecule (from 5.7 to 7.6 wt % in 90.5/7.5 and 90/10 water dilution lines, respectively).

At high water content, the effect of the food volatile molecule is more pronounced because full hydration and swelling of the cylindrical structures is expected with greater sensitivity to the guest molecules.[23]

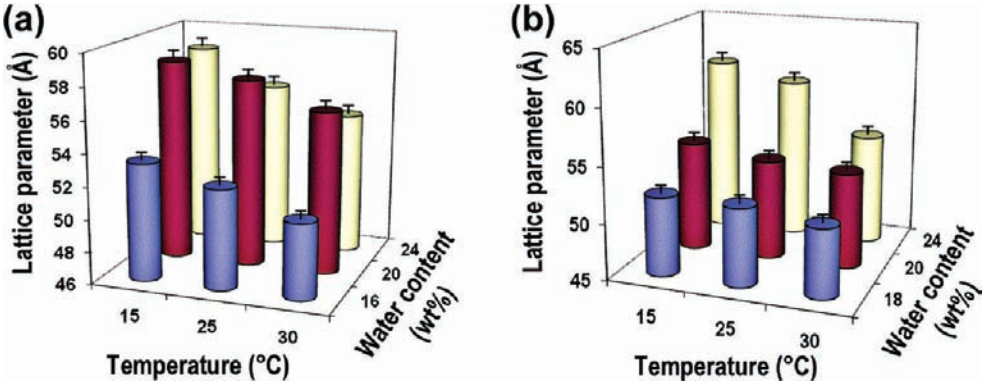

Figure 6. Effect of temperature on lattice parameter (α) in H_{II} mesophases containing (a) GMO/*trans*-4-decenal/water and (b) GMO/linalool/water at water 90/10 dilution lines.

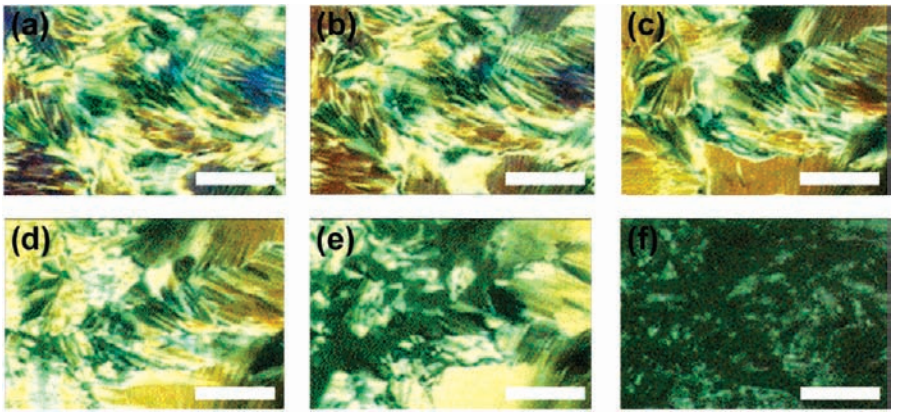

Figure 7. Polarized optical microscope images of the H_{II} liquid crystal phases containing 12.6 wt % *trans*-4-decenal at (a) 25.0, (b) 35.0, (c) 44.6, (d) 47.0, (e) 51.6, and (f) 60.1 °C at 85/15 water dilution line (GMO/*trans*-4-decenal ratio). The scale bar is 120 μm.

Temperature Dependence. In these sets of experiments, each sample of *trans*-4-decenal and linalool was cooled to 15 °C and reheated to 30 °C. In addition, lattice temperature dependence was examined by modifying the water concentration of H_{II} mesophases (containing *trans*-4-decenal or linalool in 90/10 water dilution line). In the presence of either *trans*-4-decenal or linalool, at three different water concentrations (Figure 6) a decrease in lattice parameter was observed when the temperature was raised. This temperature dependence is self-explanatory from the theory of Israelachvili et al.[14] Increasing the temperature increases the molecular mobility of the hydrocarbon chains, resulting in a demand for an increased molecular cross section. This puts a strain on the stability of the phase, which may be appeased by a mesophase transition, so that close molecular packing at the polar−nonpolar interfaces can persist while the relative volume of the nonpolar hydrocarbon region is increased. These effects increase the hydrophobic chain volume and decrease the cross-polar headgroup area. Both factors increase the CPP and decrease the lattice parameter on the assumption that the chain length decreases with an increase of the chain volume.

On the other hand, one could expect that at elevated temperatures the food volatile compound content should increase in the tails, increasing the lattice parameter. However, the opposite happened exactly as expected from Israelachvili et al.'s theory.[14] This is a good indication that the food volatile molecules are well entrapped within the H_{II} mesophase, which is exactly what will be required in food applications.

From Figure 6 we can see the water content effect on the lattice parameter. It can be seen that for *trans*-4-decenal for each temperature the lattice parameter grows with an increase of water content, but as the temperature increases, the lattice parameter increases less significantly (Figure 6a). However, for the linalool, the effect of water content is more pronounced, and as the temperature increases, the lattice parameter increases with the water content, as expected (Figure 6b).

Temperature Effect on the Morphology and Release Properties. Two samples composed of GMO/*trans*-4-decenal/water (12.3 wt % *trans*-4-decenal in 85/15 dilution line) and GMO/linalool/water (12.3 wt % linalool in 87.5/12.5 water dilution line) were studied by polarized light microscopy in the temperature range of 25−65 °C (Figure 7) (both samples contain the maximum solubilization percent of food volatile compound). At 47.0 °C, the *trans*-4-decenal sample turned fluid (Figure 7d), and at 60.1 °C (Figure 7f) the hexagonal texture disappeared, indicating total disintegration of the H_{II} mesophase.

In comparison, the linalool-based H_{II} mesophase disintegrated at *ca.* 40.8 °C (Figure 8f), where most of the hexagonal phase texture turned into a dark nonbirefringent region and the food volatile that was released was sensed.

These results indicate the transformation of the hexagonal to micellar phase and release of the food volatile compounds.

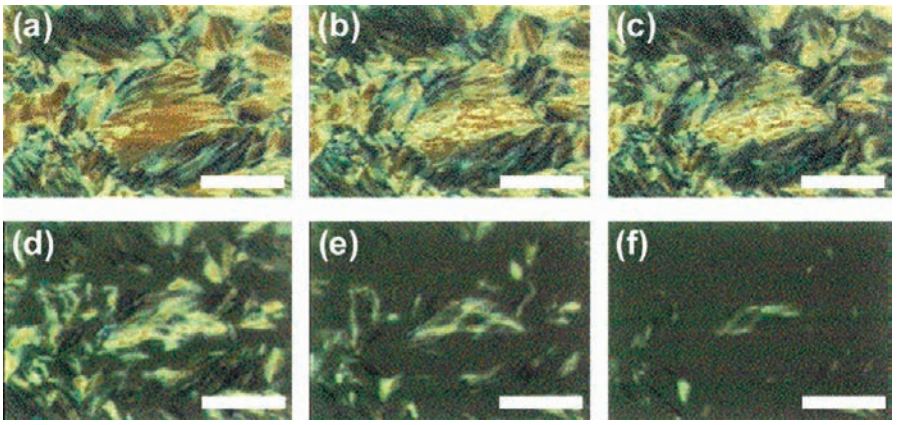

Figure 8. Polarized optical microscope images of the H_{II} liquid crystal phases containing 12.3 wt % linalool at (a) 25.0, (b) 28.7, (c) 30.6, (d) 35.1, (e) 38.3, and (f) 40.8 °C at 87.5/12.5 water dilution line (GMO/linalool ratio). The scale bar is 120 μm.

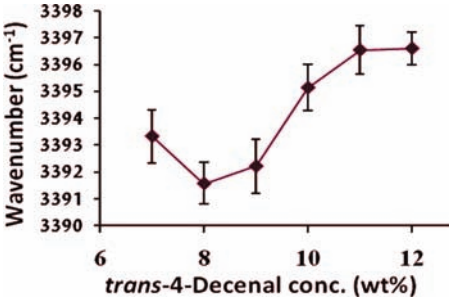

Figure 9. Wavenumber (cm^{-1}) as a function of *trans*-4-decenal concentration (7−12 wt %) of the O−H absorption modes of the surfactant molecules.

It should be noted that whereas the *trans*-4-decenal system remains intact to 60 °C, the linalool system disintegrated much earlier, in good agreement and as predicted from the lattice measurements and the differences in the H_{II} mesophase region that the two form.

Food Volatile−GMO Molecular Interactions (DSC and ATR-FTIR). The ATR-FTIR and DSC are very effective techniques to determine possible interactions between the GMO and water in the presence of the food volatile molecules and, as a result, to learn about the food volatile−GMO- molecule interactions along the solubilization process and as a function of the solubilization content.

The vibrational wavenumbers of the GMO molecules are examined in terms of the interaction of their functional groups with the water and themselves. There are three such molecular regions in the GMO molecule: the headgroups (the hydroxyl stretching and bending, region I), the interfacial moieties (the free and bound carbonyl stretchings, region II), and the lipophilic tails (the lipophilic fatty acids hydrocarbon stretching, region III).

The vibrational analysis as a function of the loading capacity of *trans*-4-decenal was carefully examined and is presented in Figures 9−11 for each region in the GMO molecule. It can be clearly seen that at low solubilization loads, the food volatile molecules do not have much of an effect on the headgroups, interfacial carbonyls, and tails. Their effects on the molecular interactions of GMO and water are very minor and not significant (no change in the wavenumbers or in the intensities). However, once the loads are large (10−12 wt % *trans*-4-decenal) the guest molecules strongly interact with the GMO.

Close examination reveals that the OH vibrations (region I) demonstrate (Figure 9) a gradual shift toward *higher* wavenumbers, which means weakening of the hydrogen bonding between the hydroxyls of the GMO and D_2O molecules. It also means that additional dehydration takes place around the headgroups in the presence of the food volatile molecules, which clearly indicates their close proximity to the headgroup, their completion on the water and D_2O molecules, and their effect on the tighter packing of the headgroups, greater effective CPP, and stabilization of the H_{II} mesophase.

A similar effect was observed on the interfacial groups of the GMO (region II). The stretching bands are divided into free and bound carbonyl (CO) vibrations. We observed a significant increase toward a larger wavenumber, from 1712 to 1719 cm^{-1}, in the bound carbonyl, which means that in the presence of large food volatile loads the GMO intra-interactions weaken because food volatile molecules are intercalated within the monoolein tails.

It is interesting to note that there was no significant change in the wavenumber of the β (Sn2) and γ (Sn1) hydroxyl stretching bands [but only a slight increase in the peak area of the symmetric and asymmetric stretching (not shown)], which indicates that the position of the hydroxyls did not change, meaning also that they continue to pack close to each other even in the presence of large loads of the food volatile molecules. Similarly, the tail interactions (region III) were not affected much by the solubilizate, which means that the food volatile molecules might be spacing the tails but not changing their dangling effect (as expected) in the oil phase.

The thermal profiles (during heating) of samples (DSC) after solubilization are the fingerprints of events that occurred in the system prior to the heating process. The subzero technique is very valuable for studying the behavior of water molecules in the inner channels as a function of the food volatile molecule load. We could clearly see that the melting point of the D_2O, which usually indicates if the water is bound to the GMO (hydrating it), moved to a higher melting temperature, which is a clear indication that in the presence of the food volatile molecules the water becomes freer. This suggests that the food volatile molecules compete on the hydration water located in the close vicinity of the headgroups. Similarly, a decrease in the enthalpy of GMO

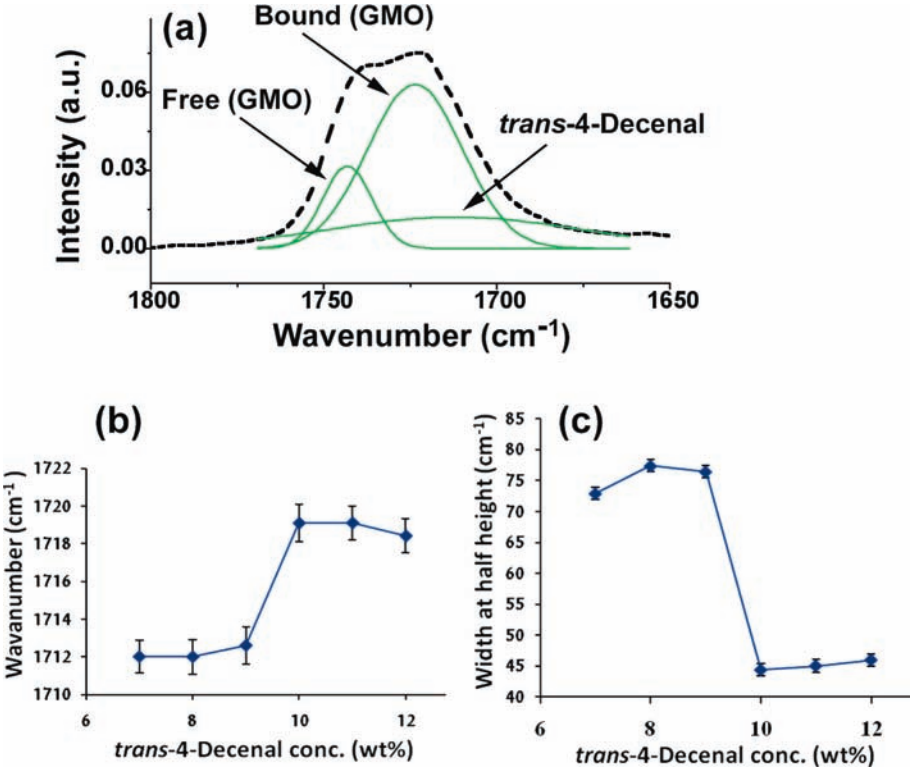

Figure 10. (a) Representative Gaussian fitting from ATR-FTIR data of the carbonyl band of GMO/*trans*-4-decenal mixture containing 50/50 surfactant/oil weight ratios demonstrating three C═O populations; "free" carbonyls (~1741 cm^{-1}) and hydrogen-bonded carbonyls (~1721 cm^{-1}) represent GMO carbonyls and *trans*-4-decenal carbonyls at ~1715 cm^{-1}. (b) Wavenumber (cm^{-1}) as a function of *trans*-4-decenal concentration (wt %) of the C═O absorption mode of the molecule. (c) Width at half-height (cm^{-1}) as a function of *trans*-4-decenal concentration (wt %) of the C═O absorption mode.

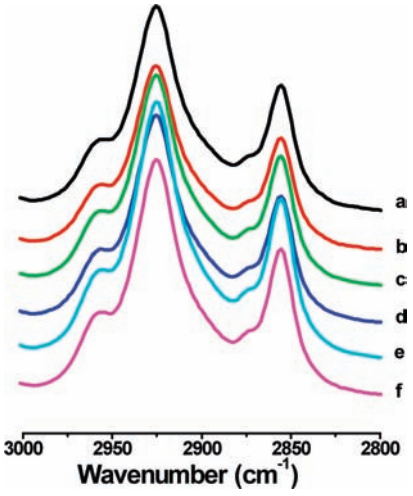

Figure 11. ATR-FTIR spectra of the H_{II} mesophases of GMO/water/*trans*-4-decenal systems with *trans*-4-decenal concentrations of (a) 7 wt %, (b) 8 wt %, (c) 9 wt %, (d) 10 wt %, (e) 11 wt %, and (f) 12 wt % in the wavenumber range of 2800−3000 cm^{-1}.

tails' endothermic peak was seen, meaning that the food volatile tails are embedded within the monoolein fatty acids (Figure 12).

The two techniques clearly indicate that the food volatile compounds at their lower solubilization loads do not interfere much with the curvature of the mesophase, but at high loads the guest molecules are interacting with GMO in the vicinity of the headgroups, modifying its CPP and stabilizing the H_{II} mesophase at room temperature.

Food Volatile Stability. The effect of the H_{II} mesophase on the stability of the food volatile compounds was tested in a preliminary study. It should be noted that both food volatile compounds when dissolved in organic solvent and left in sealed containers will be almost decomposed within 4 months (>90 wt %). Therefore, this time frame was our reference for testing the stability of the food volatile compounds in the H_{II} mesophases. It was found that the losses due to evaporation, oxidation, or decomposition were 18 and 38 wt % for *trans*-4-decenal and linalool in H_{II} mesophase, respectively. These losses were relatively smaller compared to that in solvent. It should be noted that the stability is only kinetically improved and full protection cannot be claimed.

Conclusions. In this study we demonstrated that the undesired oleic acid, oleic soaps, or TAG molecules used previously to stabilize the hexagonal mesophase at room temperature can be replaced by lipophilic food volatile compounds that facilitate the $L_\alpha \rightarrow H_{II}$ and $Q \rightarrow H_{II}$ transitions. We achieved two goals: stabilizing the hexagonal mesophase by modifying the GMO CPP (dehydrating the GMO headgroups and spacing the tails) and solubilizing large quantities of food volatile compounds in the protected domains of the H_{II} mesophase.

The solubilization capacities of four food volatile compounds, *trans*-4-decenal, linalool, 2,6-dimethyl-5-heptenal, and phenylacetaldehyde, in the GMO/water binary system were determined and found to be 12.6, 10, 12.6, and 10 wt %, respectively. The phenylacetaldehyde, even though solubilized up to 10 wt %, could not modify the CPP, and as a result only lamellar or cubic

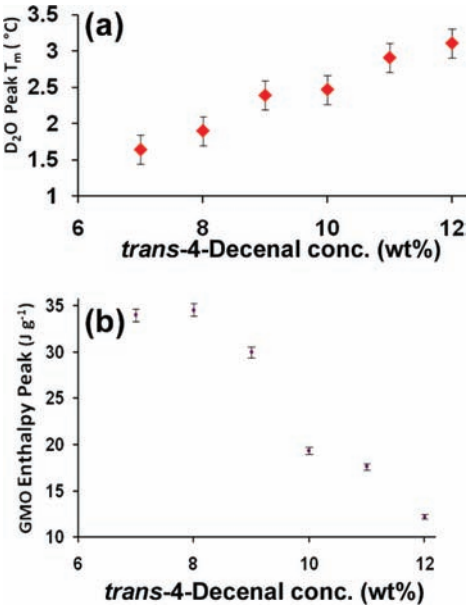

Figure 12. (a) D_2O peak melting temperature (T_m) and (b) difference of GMO peak enthalpy in the solubilization range of 7−12 wt % *trans*-4-decenal into H_{II} mesophases. These DSC temperature and enthalpy results are appropriate to ±0.2 °C and ±2%, respectively.

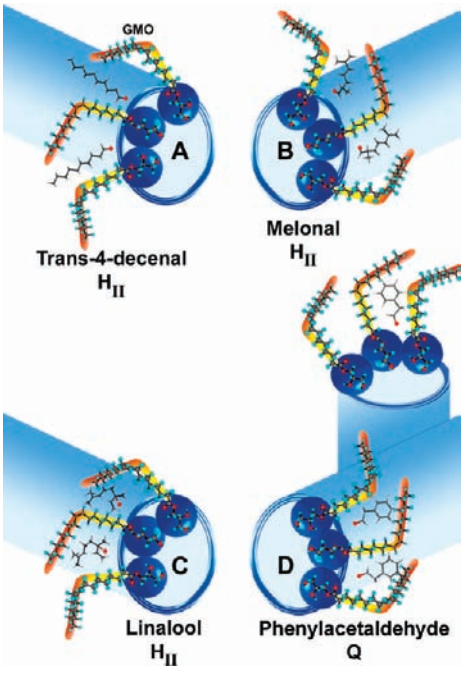

Figure 13. Schematic illustration of the solubilization loci of the four food volatile compounds within the LLC mesophase structure. Note that whereas the *trans*-4-decenal, 2,6-dimethyl-5-heptenal (melonal), and linalool are forming H_{II} mesophase at their maximum solubilization capacities, the phenylacetaldehyde is stabilizing cubic mesophase.

mesophases were formed at room temperature. Schematic representation of the food volatile compound locations within the GMO layer and the mesophase structures are shown in Figure 13. The transition to H_{II} mesophases induced by *trans*-4-decenal, 2,6-dimethyl-5-heptenal, and linalool occurs at different solubilization concentrations and different water and GMO contents depending on their chemical structure and solubilization location within the monoolein molecules. Their effect was on both the headgroups and the tails of the GMO, each based on its chemical structure.

Increasing temperature induces thermal motions of GMO tails, which caused a decrease in the lattice parameter, but at certain temperatures the H_{II} mesophase disintegrated, transforming to isotropic fluid phase (reverse micellar), which causes a food volatile release. The food volatile that has the strongest curvature effect will be resistant to temperature increase and as a result will be more protected and released at more elevated temperatures.

The FTIR results clearly indicate that low loads of food volatile compounds do not strongly interact with the GMO, but once the loads are high, the food volatile compounds are intercalated within the monoolein tails, affecting the headgroups, the interfacial moieties, and the tails and causing significant effects on lattice parameter and solubilization characteristics.

This study may open new options of using sensitive aromas both in long-term storage and in final use of food products.

AUTHOR INFORMATION

Corresponding Author

*Phone: 972-2-6586574/5. Fax: 972-2-6520262. E-mail: garti@vms.huji.ac.il.

REFERENCES

(1) Hyde, S. T. Identification of lyotropic liquid crystalline mesophases. In *Handbook of Applied Surface and Colloid Chemistry*; Holmberg, K., Ed.; Wiley: New York, 2001; Chapter 16, pp 465−504.

(2) Hyde, S. T.; Andersson, S.; Larsson, K.; Blum, Z.; Landh, T.; Lidin, S.; Ninham, B. W. Lipid self-assembly and function in biological systems. In *The Language of Shape, the Role of Curvature in Condensed Matter: Physics, Chemistry and Biology*; Elsevier: Amsterdam, The Netherlands, 1997; Chapter 5, pp 199−211.

(3) Popescu, G.; Barauskas, J.; Nylander, T.; Tiberg, F. Liquid crystalline phases and their dispersions in aqueous mixtures of glycerol monooleate and glyceryl monooleyl ether. *Langmuir* **2007**, *23*, 496–503.

(4) Clogston, J.; Rathman, J.; Tomasko, D.; Walker, H.; Caffrey, M. Phase behavior of a monoacylglycerol (Myverol 18−99K)/water system. *Chem. Phys. Lipids* **2000**, *107*, 191–220.

(5) Tiddy, G. J. T. Surfactant-water liquid-crystal phases. *Phys. Rep.−Rev. Sect. Phys. Lett.* **1980**, *57*, 1–46.

(6) Larsson, K. Cubic lipid-water phases − structures and biomembrane aspects. *J. Phys. Chem.* **1989**, *93*, 7304–7314.

(7) Pouzot, M.; Mezzenga, R.; Leser, M.; Sagalowicz, L.; Guillot, S.; Glatter, O. Structural and rheological investigation of Fd3m inverse micellar cubic phases. *Langmuir* **2007**, *23*, 9618–9628.

(8) Efrat, R.; Aserin, A.; Kesselman, E.; Danino, D.; Wachtel, E. J.; Garti, N. Liquid micellar discontinuous cubic mesophase from ternary monoolein/ethanol/water mixtures. *Colloids Surf. A* **2007**, *299*, 133–145.

(9) Larsson, K.; Fontell, K.; Krog, N. Structural relationships between lamellar, cubic and hexagonal phases in monoglyceride-water systems − possibility of cubic structures in biological-systems. *Chem. Phys. Lipids* **1980**, *27*, 321–328.

(10) Qiu, H.; Caffrey, M. The phase diagram of the monoolein/water system: metastability and equilibrium aspects. *Biomaterials* **2000**, *21*, 223–234.

(11) Misquitta, Y.; Caffrey, M. Rational design of lipid molecular structure: a case study involving the C19:1c10 monoacylglycerol. *Biophys. J.* **2001**, *81*, 1047–1058.

(12) Caffrey, M. Kinetics and mechanism of transitions involving the lamellar, cubic, inverted hexagonal and fluid isotropic phases of hydrated

monoacylglycerides monitored by time-resolved X-ray-diffraction. *Biochemistry* **1987**, *26*, 6349–6363.

(13) Lutton, E. S. Phase behavior of aqueous systems of monoglycerides. *J. Am. Oil Chem. Soc.* **1965**, *42*, 1068–1070.

(14) Israelachvili, J. N.; Mitchell, D. J.; Ninham, B. W. Theory of self-assembly of hydrocarbon amphiphiles into micelles and bilayers. *J. Chem. Soc.—Faraday Trans. 2* **1976**, *72*, 1525–1568.

(15) Mitchell, D. J.; Ninham, B. W. Micelles, vesicles and microemulsions. *J. Chem. Soc.—Faraday Trans. 2* **1981**, *77*, 601–629.

(16) Seddon, J. M. Structure of the inverted hexagonal (H_{II}) phase, and non-lamellar phase-transitions of lipids. *Biochim. Biophys. Acta* **1990**, *1031*, 1–69.

(17) Sagalowicz, L.; Leser, M. E.; Watzke, H. J.; Michel, M. Monoglyceride self-assembly structures as delivery vehicles. *Trends Food Sci. Technol.* **2006**, *17*, 204–214.

(18) Luzzati, V. X-ray diffraction studies of lipid—water systems. In *Biological Membranes, Physical Fact and Function*; Chapman, D., Ed.; Academic Press: London, U.K., 1968; Vol. 1, pp 71—123.

(19) Luzzati, V.; Gulik-Krzywicki, T. Polymorphism of lipids. *Nature* **1968**, *217*, 1028–1030.

(20) Montalvo, G.; Valiente, M.; Rodenas, E. Rheological properties of the L phase and the hexagonal, lamellar, and cubic liquid crystals of the CTAB/benzyl alcohol/water system. *Langmuir* **1996**, *12*, 5202–5208.

(21) Mezzenga, R.; Meyer, C.; Servais, C.; Romoscanu, A. I.; Sagalowicz, L.; Hayward, R. C. Shear rheology of lyotropic liquid crystals: a case study. *Langmuir* **2005**, *21*, 3322–3333.

(22) Sagalowicz, L.; Mezzenga, R.; Leser, M. E. Investigating reversed liquid crystalline mesophases. *Curr. Opin. Colloid Interface Sci.* **2006**, *11*, 224–229.

(23) Borné, J.; Nylander, T.; Khan, A. Phase behavior and aggregate formation for the aqueous monoolein system mixed with sodium oleate and oleic acid. *Langmuir* **2001**, *17*, 7742–7751.

(24) Borné, J.; Nylander, T.; Khan, A. Microscopy, SAXD, and NMR studies of phase behavior of the monoolein—diolein—water system. *Langmuir* **2000**, *16*, 10044–10054.

(25) Amar-Yuli, I.; Garti, N. Transitions induced by solubilized fat into reverse hexagonal mesophases. *Colloids Surf. B* **2005**, *43*, 72–78.

(26) Mishraki, T.; Libster, D.; Aserin, A.; Garti, N. Lysozyme entrapped within reverse hexagonal mesophases: physical properties and structural behavior. *Colloids Surf. B* **2010**, *75*, 47–56.

(27) Ben Ishai, P.; Libster, D.; Aserin, A.; Garti, N.; Feldman, Y. Influence of cyclosporine A on molecular interactions in lyotropic reverse hexagonal liquid crystals. *J. Phys. Chem. B* **2010**, *114*, 12785–12791.

(28) Cohen-Avrahami, M.; Aserin, A.; Garti, N. H_{II} mesophase and peptide cell-penetrating enhancers for improved transdermal delivery of sodium diclofenac. *Colloids Surf. B* **2010**, *77*, 131–138.

(29) Achrai, B.; Libster, D.; Aserin, A.; Garti, N. Solubilization of gabapentin into H_{II} mesophases. *J. Phys. Chem. B* **2011**, *115*, 825–835.

(30) Angelova, A.; Angelov, B.; Mutafchieva, R.; Lesieur, S.; Couvreur, P. Self-assembled multicompartment liquid crystalline lipid carriers for protein, peptide, and nucleic acid drug delivery. *Acc. Chem. Res.* **2011**, *44*, 147–156.

(31) Mohammady, S. Z.; Pouzot, M.; Mezzenga, R. Oleoylethanolamide-based lyotropic liquid crystals as vehicles for delivery of amino acids in aqueous environment. *Biophys. J.* **2009**, *96*, 1537–1546.

(32) Malmsten, M. Soft drug delivery systems. *Soft Matter* **2006**, *2*, 760–769.

(33) Drummond, C. J.; Fong, C. Surfactant self-assembly objects as novel drug delivery vehicles. *Curr. Opin. Colloid Interface Sci.* **2000**, *4*, 449–456.

(34) Mulet, X.; Kennedy, D. F.; Conn, C. E.; Hawley, A.; Drummond, C. J. High throughput preparation and characterisation of amphiphilic nanostructured nanoparticulate drug delivery vehicles. *Int. J. Pharm.* **2010**, *395*, 290–297.

(35) Kaasgaard, T.; Drummond, C. J. Ordered 2-D and 3-D nanostructured amphiphile self-assembly materials stable in excess solvent. *Phys. Chem. Chem. Phys.* **2006**, *8*, 4957–4975.

(36) Barauskas, J.; Cervin, C.; Jankunec, M.; Spandyreva, M.; Ribokaite, K.; Tiberg, F.; Johnsson, M. Interactions of lipid-based liquid crystalline nanoparticles with model and cell membranes. *Int. J. Pharm.* **2010**, *391*, 284–291.

(37) Rizwan, S. B.; Hanley, T.; Boyd, B. J.; Rades, T.; Hook, S. Liquid crystalline systems of phytantriol and glyceryl monooleate containing a hydrophilic protein: Characterisation, swelling and release kinetics. *J. Pharm. Sci.* **2009**, *98*, 4191–4204.

(38) Tilley, A.; Morton, D. A. V.; Hanley, T.; Boyd, B. J. Liquid crystalline coated drug particles as a potential route to long acting intravitreal steroids. *Curr. Drug Deliv.* **2009**, *6*, 322–331.

(39) Bitan-Cherbakovsky, L.; Yuli-Amar, I.; Aserin, A.; Garti, N. Solubilization of vitamin E into H_{II} LLC mesophase in the presence and in the absence of vitamin C. *Langmuir* **2010**, *26*, 3648–3653.

(40) Mezzenga, R.; Schurtenberger, P.; Burbidge, A.; Michel, M. Understanding foods as soft materials. *Nat. Mater.* **2005**, *4*, 729–740.

(41) Yaghmur, A.; Glatter, O. Characterization and potential applications of nanostructured aqueous dispersions. *Adv. Colloid Interface Sci.* **2009**, *147—148*, 333–342.

(42) Lynch, M. L.; Ofori-Boateng, A.; Hippe, A.; Kochvar, K.; Spicer, P. T. Enhanced loading of water-soluble actives into bicontinuous cubic phase liquid crystals using cationic surfactants. *J. Colloid Interface Sci.* **2003**, *260*, 404–413.

(43) Lopes, L. B.; Speretta, F. F. F.; Bentley, M.; Vitoria, L. B. Enhancement of skin penetration of vitamin K using monoolein-based liquid crystalline systems. *Eur. J. Pharm. Sci.* **2007**, *32*, 209–215.

(44) Angius, R.; Murgia, S.; Berti, D.; Baglioni, P.; Monduzzi, M. Molecular recognition and controlled release in drug delivery systems based on nanostructured lipid surfactants. *J. Phys.: Condens. Matter* **2006**, *18*, S2203–S2220.

(45) Lopes, L. B.; Lopes, J. L. C.; Oliveira, D. C. R.; Thomazini, J. A.; Garcia, M. T. J.; Fantini, M. C. A.; Collett, J. H.; Bentley, M. V. L. B. Liquid crystalline phases of monoolein and water for topical delivery of cyclosporin A: characterization and study of in vitro and in vivo delivery. *Eur. J. Pharm. Biopharm.* **2006**, *63*, 146–155.

(46) Vauthey, S.; Milo, C.; Frossard, P.; Garti, N.; Leser, M. E.; Watzke, H. J. Structured fluids as microreactors for flavor formation by the Maillard reaction. *J. Agric. Food Chem.* **2000**, *48*, 4808–4816.

(47) Vauthey, S.; Visani, P.; Frossard, P.; Garti, N.; Leser, M. E.; Watzke, H. J. Release of volatiles from cubic phases: monitoring by gas sensors. *J. Dispersion Sci. Technol.* **2000**, *21*, 263–278.

(48) Bauer, K.; Garbe, D.; Suburg, H. Introduction. In *Common Fragrance and Flavor Materials*; Wiley-VCH: Weinheim, Germany, 1997; pp 1—4.

(49) Lake, J. A. An iterative method of slit-correcting small angle X-ray data. *Acta Crystallogr.* **1967**, *23*, 191–194.

(50) Sjölund, M.; Rilfors, L.; Lindblom, G. Reversed hexagonal phase formation in lecithin alkane water-systems with different acyl chain unsaturation and alkane length. *Biochemistry* **1989**, *28*, 1323–1329.

(51) Kirk, G.; Gruner, S. M.; Stein, D. L. A Thermodynamic model of the lamellar to inverse hexagonal phase-transition of lipid-membrane water-systems. *Biochemistry* **1984**, *23*, 1093–1102.

(52) Gruner, S. M.; Tate, M. W.; Kirk, G. L.; So, P. T. C.; Turner, D. C.; Keane, D. T.; Tilcock, C. P. S.; Cullis, P. R. X-ray-diffraction study of the polymorphic behavior of N-methylated dioleoylphosphatidylethanolamine. *Biochemistry* **1988**, *27*, 2853–2866.

(53) Gruner, S. M. Intrinsic curvature hypothesis for biomembrane lipid-composition — a role for nonbilayer lipids. *Proc. Natl. Acad. Sci. U.S.A.* **1985**, *82*, 3665–3669.

(54) del Burgo, P.; Aicart, E.; Junquera, E. Mixed vesicles and mixed micelles of the cationic—cationic surfactant system: didecyldimethylammonium bromide/dodecylethyldimethylammonium bromide/water. *Colloids Surf. A* **2007**, *292*, 165–172.

(55) Rand, P. R.; Fuller, N. L.; Gruner, S. M.; Parsegian, V. A. Membrane curvature, lipid segregation and structural transitions for phospholipids under dual-solvent stress. *Biochemistry* **1990**, *29*, 76–87.